ACS APPLIED MATERIALS & INTERFACES

Research Article

www.acsami.org

Functionalization of Graphene Oxide Generates a Unique Interface for Selective Serum Protein Interactions

Xiaofang Tan, Liangzhu Feng, Jing Zhang, Kai Yang, Shuai Zhang, Zhuang Liu,* and Rui Peng*

Institute of Functional Nano & Soft Materials (FUNSOM), Jiangsu Key Laboratory for Carbon-Based Functional Materials & Devices, Soochow University, Suzhou, Jiangsu 215123, China

Supporting Information

ABSTRACT: Potential toxicity and risk of inducing allergy and inflammation have always been a great concern of using nanomaterials in biomedicine. In this work, we investigate the serum behaviors of graphene oxide (GO) and how such behaviors are affected by its surface modification such as PEGylation. The results show that, when incubated with human sera, unfunctionalized GO adsorbs a significant amount of serum proteins and strongly induces complement C3 cleavage (part of the complement activation cascade), generating C3a/C3a(des-Arg), an anaphylatoxin involved in local inflammatory responses, whereas PEGylated nano-GO (nGO-PEG) exhibits dramatic reductions in both protein binding in general and complement C3 activation. Moreover, we uncover that PEGylation on GO nanosheets apparently generates an interesting nanointerface, evidenced by the acquired certain selectivity and increased binding capacities of nGO-PEG toward a few serum proteins. Further mass spectrometry analysis identifies six nGO-PEG binding proteins, four of which are immune-related factors, including C3a/C3a(des-Arg). A series of Western blot analysis demonstrate that nGO-PEG binds up to 2-fold amount of C3a/C3a(des-Arg) than unfunctionalized GO, and can efficiently decrease the level of C3a/C3a(des-Arg) in treated sera, preventing the normal interaction of C3a with its receptor. In a proof-of-concept experiment, we demonstrate that nGO-PEG may serve to help eliminate the C3a/C3a(des-Arg) induced by other nanomaterials such as as-made GO, indicating a new strategy to modulate the immune responses evoked by one nanomaterial through the addition of another type of nanomaterial. Our results highlight the great importance of nanobio interface in regulating the biological effects of nanomaterials.

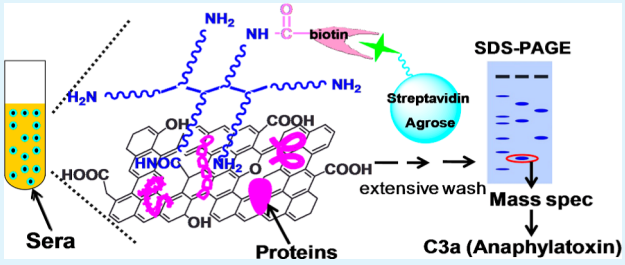

KEYWORDS: *graphene oxide, nanobio interface, serum behavior, immune response, anaphylatoxin, C3a/C3a(des-Arg)*

1. INTRODUCTION

In nanomedicine, a majority of imaging nanoprobes or therapeutic nanoparticles are usually intravenously administrated directly into the circulating blood. The interactions between serum proteins and foreign nanomaterials, as well as the possible immune responses and complement activations, are thus fundamental issues in the development of nanomedicine.[1−6] Previous studies have uncovered that certain nanomaterials bound with proteins could result in protein aggregation,[7,8] protein disfunction,[9] blood coagulation,[3] and the exposure of normally embedded epitopes to the local environment.[10] Whether and how the immune system recognizes and reacts to the administrated nanomaterials is also regarded as a major problem that regulates both safety and functions of nanotheranostics.[11−13]

The complement system is a phylogenetically ancient part of the innate immune system, consisting of a group of small proteins found in the blood which can mediate opsonization of bacteria, activation of inflammation, as well as clearance of immune complexes.[14] Complement activation occurs through three different pathways: the classical, lectin and alternative pathways, all of which lead to C3 cleavage into two activation products, C3a and C3b. The larger fragment, C3b, triggers a cascade of further cleavage and activation events leading to the formation of the cell-killing membrane attack complex (MAC),[15] whereas the smaller one, C3a, functions as an anaphylatoxin to mediates chemotaxis, local inflammatory responses, and smooth muscle contraction, as well as enhances vascular permeability. C3a is then quickly processed to lose its C-terminal arginine, generating acylation stimulating protein (ASP, also referred to as C3a(des-Arg)),[16] an adipogenic cytokine involved in the pathogenesis of obesity. Increased levels of ASP have been reported in patients with obesity, diabetes, and cardiovascular diseases.[17] Because of the high proinflammatory potential of C3a and its relationship to a number of diseases,[18−21] it is particularly important to study complement C3 cleavage and any variations in blood C3a level when encountered with nanomaterials.

Graphene and its derivatives such as graphene oxide (GO), are two-dimensional (2D) sp^2 carbon nanomaterials and have attracted tremendous attention due to their intriguing physical, chemical and mechanical properties.[22−25] In recent years, the

Received: November 14, 2012
Accepted: January 29, 2013
Published: January 29, 2013

biomedical applications of graphene derivatives have also been widely explored by a large number of groups.[26−37] Various graphene-based diagnostic platforms have been fabricated for in vitro or ex vivo detection of biomolecules with great sensitivity.[38] With ultrahigh surface area, functionalized derivatives are able to serve as novel nanocarriers for loading and intracellular delivery of both small drug molecules and biomarcomolecules such as DNA and small interfering RNA.[39−50] With strong absorbance in the near-infrared region, GO or reduced GO (rGO) after coating with biocompatible polymers such as polyethylene glycol (PEG) can be utilized as cancer therapeutic agents for in vivo photothermal ablation of tumors in animal experiments with high efficacy.[43,51−56] Imaging guided cancer therapy using GO-based nanocomposite as theranostic probes has also been demonstrated in our latest work.[42] Graphene-based nanomedicine appears to be promising and may bring novel opportunities for future disease diagnosis and treatment.

Potential toxicity has always been a great concern of using nanomaterials in biomedicine. Although a number of previous reports have shown that, different from pristine graphene or as-made GO which exhibit noticeable in vitro and in vivo toxicity,[29,57,58] appropriately functionalized GO does not possess obvious toxicity to animals, and its in vivo behaviors are closely relevant to its surface chemistry and size,[59−64] how GO and functionalized nano-GO (e.g., nGO-PEG) interact with the immune system, particularly proinflammatory factors, is a crucial question in the future exploration of GO-based materials in nanomedicine, and still remains to be addressed. In this work, we start to look into the above question by investigating and comparing the interactions of serum proteins with GO and nGO-PEG, the latter of which has ultrasmall sizes and is functionalized by a 10 kDa amine-terminated six-arm-branched PEG polymer (10k-6*br*-PEG-NH_2).[65] Interestingly, unlike GO, which adsorbs a significant amount of serum proteins in a nonspecific manner, nGO-PEG not only exhibits reduced protein binding in general but also certain selectivity and increased affinities toward a few proteins. Six nGO-PEG binding proteins are identified, and four of them are immune-related factors, including C3a/C3a(des-Arg). Further comparison of the sera treated with GO and nGO-PEG show that nGO-PEG is able to induce certain level of complement C3 cleavage, but to a much less extent than GO does. More importantly, nGO-PEG possesses up to 2-fold binding capacity toward C3a/C3a(des-Arg) than GO does, resulting in dramatically decreased level of C3a/C3a(des-Arg) in treated sera. Remarkably, this unique property of nGO-PEG enables it to effectively modulate C3a/C3a(des-Arg) content when complement C3 is activated by foreign objects such as unfunctionalized GO. This novel phenomenon suggests the potential use of nGO-PEG to attenuate the consequences of complement C3 activation induced by other nanomaterials for better biocompatibility.

2. EXPERIMENTAL SECTION

2.1. Preparation and Characterization of GO and nGO-PEG. GO and nGO-PEG were prepared as previously described.[52,65] Briefly, GO was synthesized from graphite following a modified Hummers method. nGO-PEG was prepared by conjugating 10k-6*br*-PEG-NH_2 (Sunbio Inc., South Korea) to as made GO via amide formation. The reaction was then filtered through Amicon Ultra Centrifugal Filters with molecular weight cutoff (MWCO) of 100 kDa (Millipore, Carrigtwohill, co. cork, Ireland) and repeatedly washed using ultrapure water to remove excess PEG polymer.

The concentration of nGO-PEG was calculated using its absorbance at 230 nm (mass extinction coefficient of 65 mg/mL/cm).[44] Both as made GO and nGO-PEG were characterized by FT-IR using Hyperion series spectrometer (Bruker), AFM analysis using a MutiMode V AFM (Veeco), and DLS on a Zen3690 (Malvern) at the scattering angle θ = 17°.

2.2. Preparation of Human Serum. Human serum samples were prepared from twenty healthy male volunteers (aged 23−45 years) according to approved local protocols. Blood drawn from each individual was allowed to clot at room temperature, and serum was extracted, pooled, and stored in aliquots at −80 °C. Immediately before use, serum samples were thawed on ice.

2.3. Serum Protein Adsorption on Unfunctionalized GO. 0.4 mg/mL GO was incubated with undiluted sera (sample:sera = 1:1 v/v) at 37 °C for 1 h. GO and bound proteins were precipitated by centrifugation at 21 000 g for 30 min at 4 °C. Pellets were carefully washed four times with ice-cold washing buffer (phosphate buffer (1 × PBS), pH 7.5, 800 mM KCl, 0.01% TWEEN 20), and resuspended in 1× Laemmli loading buffer.[66]

2.4. Biotin-streptavidin Pull-down Assay. One mg/mL PEG polymer and 0.4 mg/mL nGO-PEG were biotinylated at the terminal amines by addition of 0.5 mM NHS-biotin (Sigma-aldrich, St. Louis, MO, USA), and stirred at room temperature overnight. Excess NHS-biotin was removed by filtration through Amicon Ultra Centrifugal Filters (MWCO 100 kDa) and washed over eight times using 1 × PBS (pH 7.5). The concentration of biotinylated nGO-PEG was calculated using its absorbance at 230 nm with the same mass extinction coefficient.

Biotin-streptavidin pull-down assay were carried out by incubating different samples (0.05 mg/mL biotinylated nGO-PEG, 0.05 mg/mL nGO-PEG, 0.25 mg/mL biotinylated PEG or saline as control) with undiluted sera (sample:sera = 1:1 v/v) at 37 °C for 1 h, chilled on ice for 20 min, and then mixed with 50 μL streptavidin agarose beads (Pierce/Thermo Scientific, Rockford, USA). Following incubation at 4 °C for 1 h, beads and bound proteins were precipitated by brief centrifugation, washed three times with 750 μL of ice-cold washing buffer, and resuspended in 50 μL 2 × Laemmli loading buffer. Protein samples were separated on 12% sodium dodecyl sulfate polyacrylamide gel electrophoresis (SDS-PAGE) and analyzed by silver staining, Coomassie Blue staining for further mass spectrometry identification, or Western blot using a mouse monoclonal antibody raised against human C3a/C3a(des-Arg) (Santa Cruz Biotechnology Inc., Santa Cruz, CA, USA).

2.5. Mass Spectrometry Protein Identification. Individual protein bands were excised and subjected to in-gel trypsin digestion. Peptide mixtures were analyzed by LC-MS/MS using a high performance liquid chromatography system (Michrom BioResources Inc.) coupled to a Finnigan LTQ ion trap mass spectrometer (Thermo Fisher Scientific, Waltham, MA) equipped with a nanospray ion source, in the Instrumental Analysis Center at Shanghai Jiaotong University. Mass spectral data were used to interrogate the Swiss-Prot and NCBInr protein databases for statistically significant protein matches.

2.6. In vitro Complement C3 Activation Assay. Complement activation reactions were carried out by mixing different material samples or saline as indicated in the text with undiluted sera (sample:sera = 1:4 v/v), followed by incubation at 37 °C for 1 h. Reactions were then terminated on the ice. Following separation on 12% SDS-PAGE, complement C3 cleavage product C3a/C3a(des-Arg) was analyzed by Western blot using antihuman C3a/C3a(des-Arg) antibody. For preparation of the C3a/C3a(des-Arg)-elevated serum samples, same activation procedure was used except that the reactions were incubated at 37 °C for 30 min.

2.7. Calcium Flux Assay. U937 cells (human macrophage cell line, a gift from Dr. Yun Zhao) were cultured in RPMI 1640 medium supplemented with 10% fetal bovine serum (FBS). The intracellular Ca^{2+} changes were measured using fura-2/AM fluorescence assay (sigma-Aldrich, St. Louis, MO, USA) as previously described.[67] Briefly, 1 × 10^6 U937 cells were incubated at 37 °C in the dark with 3 μM fura-2/AM. After 30 min incubation, cells were washed twice,

resuspended in Hank's Balanced Salt Solutions (HBSS, 137 mM NaCl, 5 mM KCl, 1.3 mM $CaCl_2$, 0.8 mM $MgSO_4$, 0.6 mM Na_2HPO_4, 0.4 mM KH_2PO_4, 3.0 mM $NaHCO_3$, 5.6 mM glucose, pH 7.4), stimulated with different serum samples or serum pull-down samples as indicated in the text, and then immediately analyzed using a Varioskan Flash Microplate Reader (Thermo Fisher Scientific, Waltham, MA). The free cytosolic Ca^{2+} concentrations were calculated as previously described.[67]

3. RESULTS AND DISCUSSION

3.1. Preparation and Functionalization of GO Nanosheets. GO was prepared from graphite following the modified Hummer's protocol.[40,42] nGO-PEG was synthesized from GO sheets by covalent conjugation with 10k-6*br*-PEG-NH_2 via amide formation as previously described,[65] and confirmed by zeta potential shift (from −47.6 mV to −13.5 mV, Figure 1a) as

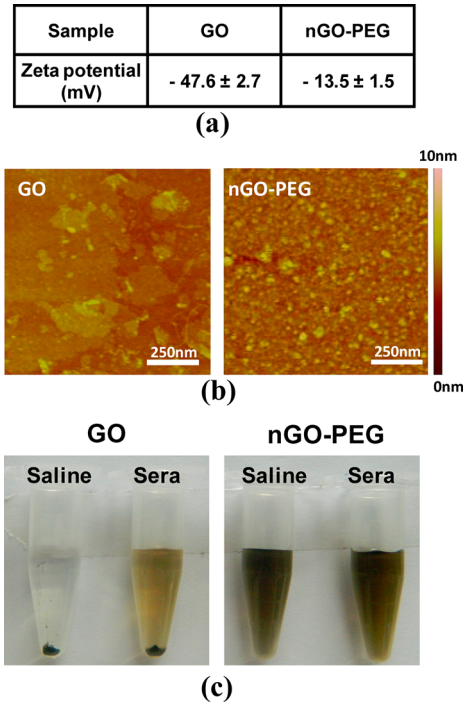

Figure 1. Characterization of GO and nGO-PEG used in the study. (a) Zeta potential and (b) AFM images of GO and nGO-PEG. (c) Photos of GO and nGO-PEG at the same concentration (0.08 mg/mL) in saline and human sera after centrifugation at 21 000 g for 5 min.

well as infrared (IR) spectra (see the Supporting Information, Figure S1). Atomic force microscope (AFM) images showed that different from GO with large sizes up to a few μm, nGO-PEG nanosheets were mainly single- or double-layered ultrasmall sheets with a size range of 10−50 nm (Figure 1b). As shown in Figure 1c, the majority of GO precipitated out after centrifugation in normal saline (0.9% NaCl) or human sera at 21 000 g for 5 min, whereas no noticeable aggregation was observed in nGO-PEG samples under the same conditions, demonstrating its greatly improved dispersibility in physiological solutions.

3.2. Alterations in the Capacity and Selectivity of GO Nanosheets for Serum Proteins upon PEGylation. As a common functionalization approach, PEGylation is widely used in nanobiotechnology to increase biocompatibility of nanomaterials and decrease nonspecific adsorption of biomolecules on their surfaces.[5,68−71] We first investigated the adsorption of serum proteins on GO and how PEGylation affects such interactions. Unfunctionalized GO was incubated with human sera at 37 °C for 1 h, and then precipitated by centrifugation at 21 000 g. Given the excellent dispersibility in serum without precipitation even under harsh centrifugation, nGO-PEG was biotinylated at PEG terminal amines (nGO-PEG-biotin) before incubation with sera, and then pulled down using streptavidin agarose beads (Figure 2a) for separation and further analysis. To ensure specificity, both biotinylated PEG (PEG-biotin) and nGO-PEG without biotinylation were used as controls in the biotin-streptavidin pull-down reactions. As expected, after centrifugation, the color of collected beads turned black only in the nGO-PEG-biotin containing reaction but not in the control reaction which contained nGO-PEG without biotinylation (data not shown), suggesting successful and specific separation of nGO-PEG-biotin using streptavidin agarose beads in our assay.

After extensive washing (800 mM KCl in PBS) of GO precipitates and beads-bound nGO-PEG-biotin collected from sera, tightly bound proteins were eluted and analyzed by SDS-PAGE (Figure 2b). The majority of serum proteins coprecipitated with GO, most likely via nonspecific hydrophobic adsorptions, whereas PEGylation significantly decreased the total amount of protein binding (compare lane 1, lane 2, and lane 4), similar to previous reports.[2,5,72,73] Interestingly, PEGylation altered protein binding selectivity as well. As shown in Figure 2b, besides several protein bands common to all pull-down reactions, which were disregarded as nonspecific ones, a number of protein bands presented only in the nGO-PEG-biotin lane (compare lane 4 with lane 3, lane 5, and lane 6), suggesting highly selective protein binding on nGO-PEG. Among these specific bands, at least four of them (indicated by arrow heads) appeared in rather increased amounts compared to those adsorbed on unfunctionalized GO, suggesting enhanced affinities and/or specificities toward nGO-PEG.

3.3. Selective Binding of Immune Factors to nGO-PEG. Two of the above protein bands with better separation and clean background (Figure 2b, indicated by solid arrow heads) were selected for further identification by mass spectrometry (LC-MS/MS, see the Supporting Information, Table S1). Six proteins, including four glycoproteins, were identified (Figure 2b and Table 1). Band No. 1, which migrated at around 9 kDa, contained platelet factor 4 (PF4),[74] vitronectin (10 kDa subunit V10),[75] and C3a/C3a(des-Arg). Noting that C3a and C3a(des-Arg) are hard to distinguish for C3a(des-Arg) is shorter by only one arginine at the C-terminus. The band of approximately 34 kDa (Band No. 2) contained clusterin (α chain and β chain),[76] thrombin,[77] and histidine-rich glycoprotein (HRG, N-terminal domain).[78] Three of the glycoproteins, clusterin, HRG, and vitronectin, despite their various physiological functions, have all been implicated in regulating immune responses: clusterin and vitronectin, in particular, are both regulators of the complement mediated cytolysis. Therefore, together with C3a, an important intermediate product of the complement activation cascade triggering immune responses, four out of six identified nGO-PEG-binding proteins are related to the body's defense system, implicating possible effects of nGO-PEG on the immune system, especially on complement and other related processes. The other two identified proteins (PF4 and thrombin) are two coagulation factors that, during the blood clotting process, are released from platelet and generated from its proenzyme, respectively.[74,77] Rather abundant amounts of

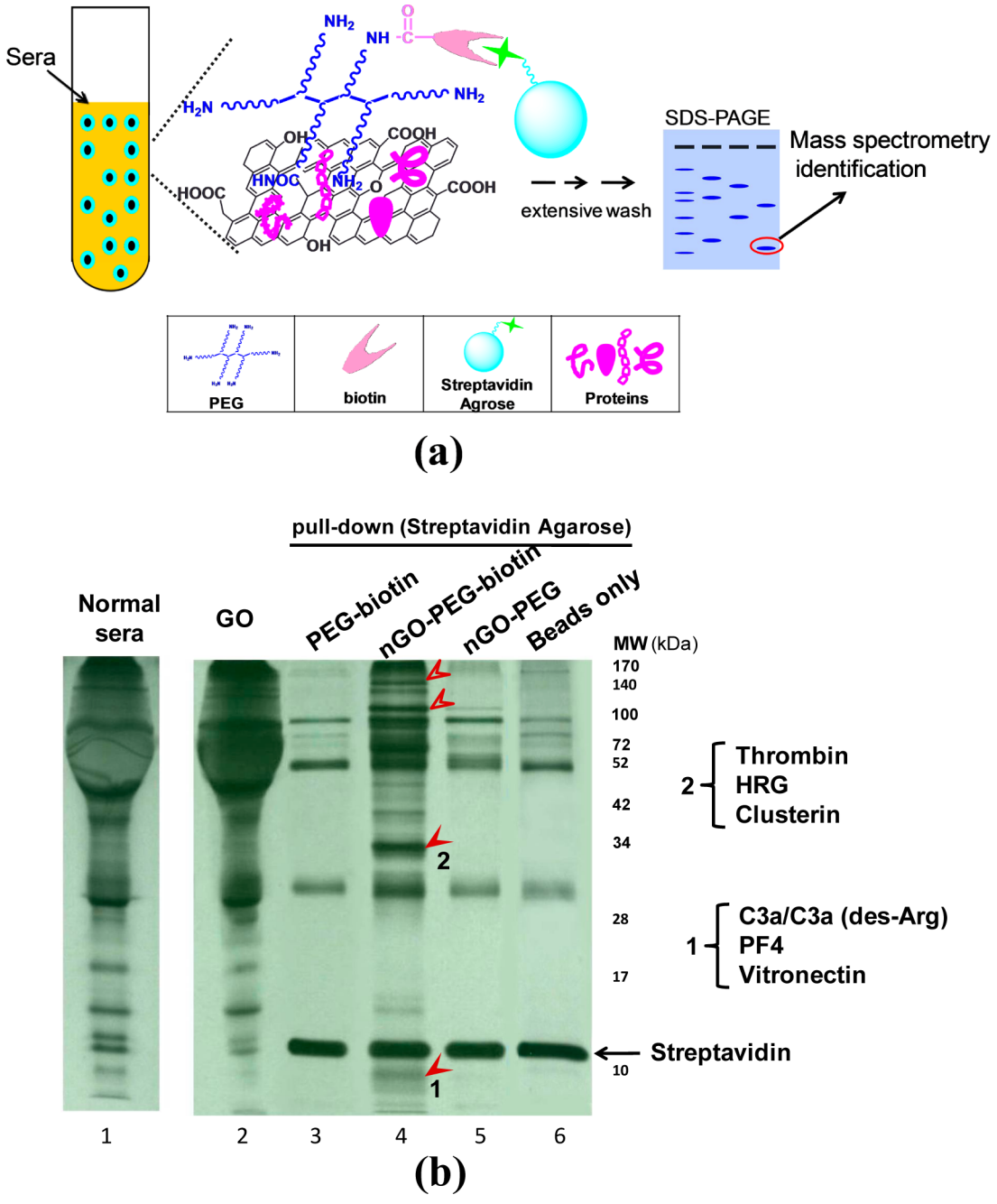

Figure 2. PEGylation of GO altered its interactions with serum proteins. (a) Biotin-streptavidin pull-down assay. nGO-PEG was biotinylated at PEG terminal amines before incubation with sera at 37 °C for 1 h, and then pulled down using streptavidin agarose beads followed by extensive washing (800 mM KCl in PBS). Bound proteins were eluted, separated by 12% SDS-PAGE, and then analyzed by silver staining or LC-MS/MS identification. (b) Silver staining of serum proteins associated with different GO nanosheets. Lane 1: normal human sera used in the study. Lane 2: unfunctionalized GO was incubated with human sera at 37 °C for 1 h, and then precipitated by centrifugation at 21,000 g, followed by washing using 800 mM KCl in PBS. Bound proteins were eluted, separated by 12% SDS-PAGE, and silver stained. Lane 3–6: biotin-streptavidin pull-down assay was performed using biotinylated PEG (PEG-biotin, lane 3), biotinylated nGO-PEG (nGO-PEG-biotin, lane 4), nGO-PEG without biotinylation (nGO-PEG, lane 5), and saline as control (Beads only, lane 6), respectively. Four protein bands appeared in obviously higher densities in lane 4 than in lane 2 are marked by arrow heads, among which the two bands labeled by solid arrowhead #1 and #2 were cut out and identified by LC-MS/MS, and results are listed on the right.

thrombin were recovered in the second band, as indicated by the large number of its peptide hits, possibly because of its "trypsin-like" nature[79] and nGO-PEG's known association with trypsin in our previous report.[65] However, the association of thrombin and PF4 with nGO-PEG in serum might be a pseudo effect and is unlikely to reflect the actual events that happen in blood, since their circulation levels are extremely low, but increase by more than 3 orders of magnitude during serum preparation (clotting).[74,80,81]

The LC-MS/MS data further revealed the high selectivity of nGO-PEG, because among the many serum proteins or their subunits that migrate at around 9 kDa or 34 kDa on reducing SDS-PAGE, only six of them were identified to associate with nGO-PEG. Furthermore, these identified proteins possess

Table 1. nGO-PEG-Associated Serum Proteins

protein	band	glycoprotein	swiss-port	pI	peptide hits	function
C3a/C3a(des-Arg)	1	no	P01024	9.69	12	complement C3 activation products; proinflammatory/adipogenic cytokine.
Vitronectin	1	yes	P04004	5.46	17	inhibit complement MAC formation; promote cell adhesion and spreading.
Clusterin	2	yes	P10909	5.85	3	part of the complement MAC; protects cells against apoptosis and complement-mediated cytolysis.
HRG	2	yes	P04196	7.09	9	multifunctional; regulate immune complex and pathogen clearance, cell adhesion, angiogenesis, coagulation and apoptosis
PF4	1	no	P02776	8.72	11	released from activated platelets; heparin binding; promote coagulation.
Thrombin	2	yes	P00734	5.55	376	serine protease; coagulation cascade; catalyze coagulation-related reactions

different isoelectric points (pIs), ranging from 5.46 to 9.69 (Table 1), suggesting that their binding to PEGylated GO surface is likely through some specific interactions other than simple nonspecific electrostatic attraction. Take Band No. 1 for example, the anaphylatoxin family consists of three 9 kDa homologous proteins (C3a, C4a, and C5a), which are all generated enzymatically during complement activation, possessing similar functions and close pIs, yet only C3a was identified here. The selectivity of nGO-PEG for C3a/C3a(des-Arg) was further analyzed and confirmed by Western blot using monoclonal antibody against C3a/C3a(des-Arg). As shown in Figure 3, compared to unfunctionalized GO that bound both

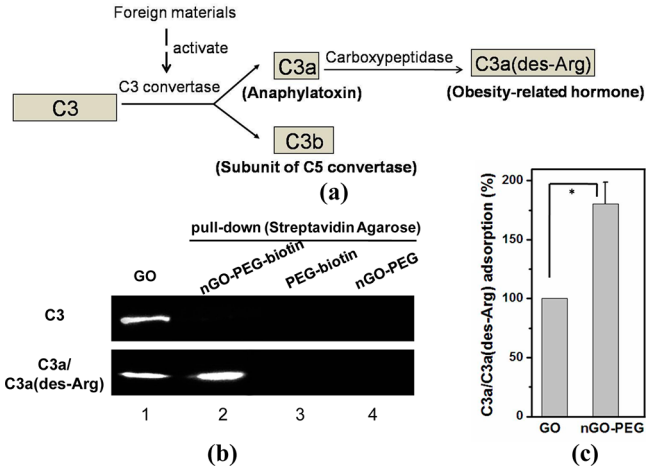

Figure 3. Selective binding of nGO-PEG to C3a/C3a(des-Arg). (a) Diagram of the complement C3 activation pathway. (b) Samples of serum proteins bound to GO and nGO-PEG were prepared as described in Figure 2, followed by 12% SDS-PAGE and Western blot analysis using a monoclonal antibody against human C3a/C3a(des-Arg). (c) Relative quantification of the C3a/C3a(des-Arg) levels in (b). Error bars represent the standard deviation (n = 3). *P < 0.005.

C3a/C3a(des-Arg) and C3 with no apparent difference, the same amount of nGO-PEG exhibited almost no detectable binding to C3, but rather nearly 2-fold binding to C3a/C3a(des-Arg). Since the peptide sequence of C3a/C3a(des-Arg) is also present in C3, the selective binding of C3a/C3a(des-Arg) over C3 by nGO-PEG indicate that the differences in the overall conformations and secondary structures of C3 and C3a/C3a(des-Arg) might contribute to their interactions with nGO-PEG. Taken together, the above results all demonstrate selective and efficient association of GO nanosheets with certain immune factors after the PEGylation, which clearly changes the surface chemistry, resulting in altered nanobio interface for protein binding.

3.4. Complement C3 Cleavage Induced by GO Nanosheets. The complement system helps clear foreign objects (e.g., pathogens) from blood in a process beginning with its activation by these intruders or relating triggers. Since the three different complement activation pathways all lead to enzymatic cleavage of complement factor C3 to C3a and C3b, our finding that PEGylation can effectively alter the interactions of C3 and C3a/C3a(des-Arg) with GO and nGO-PEG suggests that it might affect the C3 cleavage process as well. To investigate whether GO and nGO-PEG can induce complement C3 cleavage, and whether PEGylation could affect such a process, GO, nGO-PEG, coating polymer (PEG), and zymosan (a glucan known to activate complement,[82] as positive control) were incubated with human sera at 37 °C, respectively, and the serum level of C3a/C3a(des-Arg) in each reaction, which represents the degree of C3 splitting, was analyzed by Western blot (Figure 4). Compared to saline treatment (negative

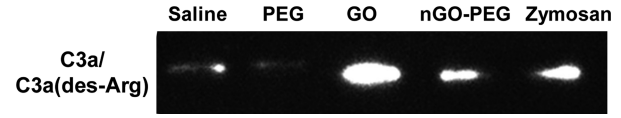

Figure 4. Reduced complement C3 cleavage after PEGylation. Human sera was incubated with 80 μg/mL GO, 80 μg/mL nGO-PEG, 0.5 mg/mL PEG, and 10 mg/mL zymosan (as positive control) at 37 °C, respectively, and C3 cleavage in each reaction was analyzed by Western blot using antihuman C3a/C3a(des-Arg) antibody.

control), coating polymer PEG alone did not cause activation of C3 even at high concentrations, consistent with its good biocompatibility. Treatment with unfunctionalized GO resulted in the largest increase in C3a/C3a(des-Arg) level among all reactions, showing its dramatic stimulatory effect on C3 cleavage. In the case of nGO-PEG treatment, although there was a significant reduction in the level of C3a/C3a(des-Arg) comparing to GO treatment, nGO-PEG was still able to induce C3 cleavage to an extent similar to zymosan, demonstrating moderate improvement of complement compatibility by this type of PEGylation.

3.5. High Binding Capacity of nGO-PEG toward C3a/C3a(des-Arg). We have shown that nGO-PEG, when incubated with human sera at 37 °C, can not only trigger complement C3 cleavage, but also selectively bind to one of the cleavage products C3a and/or its derivative C3a(des-Arg). Two questions thus arise as whether C3 cleavage induce by nGO-PEG is required for its binding to C3a/C3a(des-Arg), and what is the ultimate effect on serum C3a/C3a(des-Arg) level after nGO-PEG treatment. To address the first question, we bound nGO-PEG-biotin to streptavidin agarose first to prepare nGO-PEG-conjugated agarose beads. These conjugated beads were

then incubated with sera at 4 °C, under which condition no complement C3 activation would occur. Normal streptavidin agarose beads were used as control. After incubation, beads and bound proteins were removed from each reaction. C3a/C3a(des-Arg) remained in the supernatant as well as its total amount before beads removal were analyzed by Western blot (Figure 5a). Total levels of C3a/C3a(des-Arg) in both

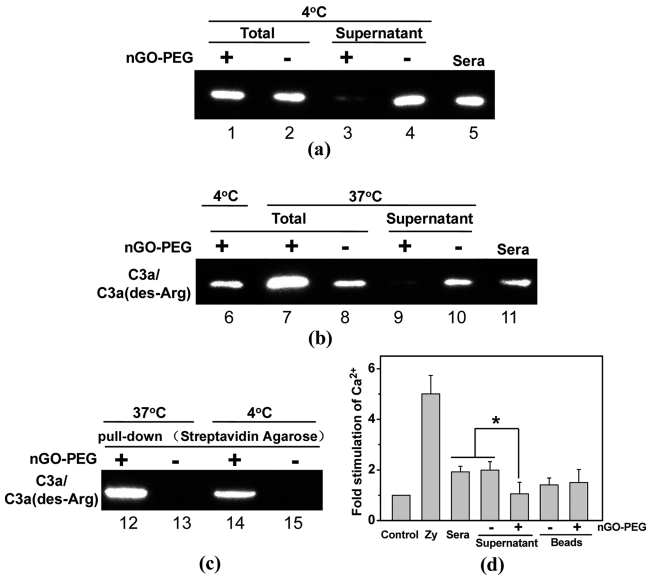

Figure 5. High binding capacity of nGO-PEG toward C3a/C3a(des-Arg) and inhibition of C3a function by nGO-PEG binding. Pull-down assay was performed using either nGO-PEG-conjugated streptavidin agarose beads (+) or unconjugated streptavidin agarose beads (−) at indicated incubation temperature: (a) 4 and (b) 37 °C, respectively. After sera incubation, fractions were collected before (Total) and after (Supernatant) beads removal. The amount of C3a/C3a(des-Arg) in each fraction was analyzed by Western blot using antihuman C3a/C3a(des-Arg) antibody. (c) Western blot of C3a/C3a(des-Arg) associated with streptavidin agarose beads after pull-down. (d) Regulation of free cytosolic Ca^{2+} in U937 cells. Fura-2/AM-loaded U937 cells were incubated with indicated serum samples, samples from the 37 °C pull-down assay, or HBSS buffer as the control. The changes of cytosolic Ca^{2+} concentrations were measured immediately as described in the Experimental Section. + represents 33 μg/mL beads-conjugated nGO-PEG in the reaction. Zy represents C3a-elevated sera prepared by pretreatment with 10 mg/mL zymosan at 37 °C. Error bars represent the standard deviation (n = 4). *P < 0.05.

reactions (lane 1 and lane 2) were the same as that in normal sera (lane 5), confirming that no C3 cleavage was induced during incubation. Majority of the C3a/C3a(des-Arg) was found to coprecipitate with nGO-PEG-conjugated beads (lane 14), leaving trace amount of it in treated supernatant (lane 3), hence its binding to nGO-PEG does not require C3 activation. Similar experiments were performed to address the second question, except that the incubation of sera with either the control beads (normal streptavidin agarose beads, nGO-PEG -) or nGO-PEG-conjugated beads (nGO-PEG +) was carried out at 37 °C instead of 4 °C (Figure 5b, 5c). At 37 °C, normal streptavidin agarose beads (nGO-PEG -) did not activate complement C3 (compare lane 8 with lane 6 and lane 11). Even though some C3a/C3a(des-Arg) was induced by nGO-PEG (compare lane 7 with lane 6 and lane 8), the binding capacity of nGO-PEG to C3a/C3a(des-Arg) was high enough (lane 12) to clear not only the newly generated C3a/C3a(des-Arg), but also most of the pre-existing ones from sera, ultimately resulting in the significantly decreased level of C3a/C3a(des-Arg) in nGO-PEG treated supernatant (lane 9).

3.6. nGO-PEG as A Potential Inhibitor of C3a Function. C3a functions through binding to its receptor C3aR (a cell surface G protein-coupled receptor) in target cells to mediate chemotaxis and inflammatory responses.[83] The binding of C3a to C3aR induces a quick rise in free cytosolic Ca^{2+}, which can be analyzed using U937 cells, a human macrophage cell line expressing C3aR.[67,84] As shown in Figure 5d, normal sera caused about 2-fold increase in the free cytosolic Ca^{2+} level in U937 cells, whereas C3a-elevated sera, prepared by pretreatment with 10 mg/mL zymosan at 37 °C, greatly stimulated intracellular Ca^{2+} flux, resulting in a 5-fold rise of free cytosolic Ca^{2+}.

To further investigate the effect of nGO-PEG binding on the activity of C3a, we prepared nGO-PEG-bound C3a and separated it from sera as described in parts b and c in Figure 5 using nGO-PEG-conjugated beads (nGO-PEG +) at 37 °C. For comparison, normal streptavidin agarose beads (nGO-PEG −) were used in the mock reaction. The beads with associated proteins as well as the supernatants were then tested for their abilities to stimulate intracellular Ca^{2+} flux in U937 cells (Figure 5d). The supernatant after nGO-PEG-beads separation showed significantly decreased calcium stimulation compared to both normal sera and the mock supernatant (nGO-PEG -), and the cytosolic Ca^{2+} level remained almost the same as that in the control U937 cells, consistent with the barely detectable C3a/C3a(des-Arg) level in Western blot analysis (Figure 5b, lane 9). Although after pull-down a large amount of C3a/C3a(des-Arg) was found to associated with nGO-PEG (Figure 5c, lane 12), these nGO-PEG-bound C3a exhibited little calcium stimulatory activity, evidenced by the similar cytosolic Ca^{2+} levels observed in cells treated with nGO-PEG-conjugated beads (nGO-PEG +) and normal streptavidin agarose beads (nGO-PEG −). Our results suggest that the binding of nGO-PEG to C3a can suppress C3a function by interfering with the interaction between C3a and its receptor C3aR.

3.7. nGO-PEG as A Potential Regulator of C3a/C3a(des-Arg) Level. C3a is an anaphylatoxin causing chemotaxis, local inflammatory responses, and allergic-like reactions, while its derivative C3a(des-Arg) is an adipogenic cytokine involved in the pathogenesis of obesity. Therefore, compare to other nanomaterials that can induce similar level of complement C3 activation, nGO-PEG might have lower risk of causing immune responses, because it can retain the anaphylatoxin C3a produced from C3 cleavage and prevent the normal interaction between C3a and its receptor. Furthermore, given its high C3a/C3a(des-Arg) binding capacity as well as the fact that its binding to C3a/C3a(des-Arg) and C3 activation are two separate events, nGO-PEG should also be able to bind C3a/C3a(des-Arg) generated by other complement-activating materials, adjusting the serum C3a/C3a(des-Arg) level. As a proof-of-concept demonstration, two types of complement-activating materials, zymosan (a natural glucan from yeast) and unfunctionalized GO (a synthetic nanomaterial), were incubated with sera at 37 °C, respectively. These C3a/C3a(des-Arg)-elevated sera were then treated with nGO-PEG-conjugated beads. As shown in Figure 6, nGO-PEG treatment successfully restored the basal C3a/C3a(des-Arg) level in GO-treated supernatant (lane 3), and for sera incubated with the relatively weaker activator, zymosan, nGO-PEG treatment led to a decrease of C3a/C3a(des-Arg)

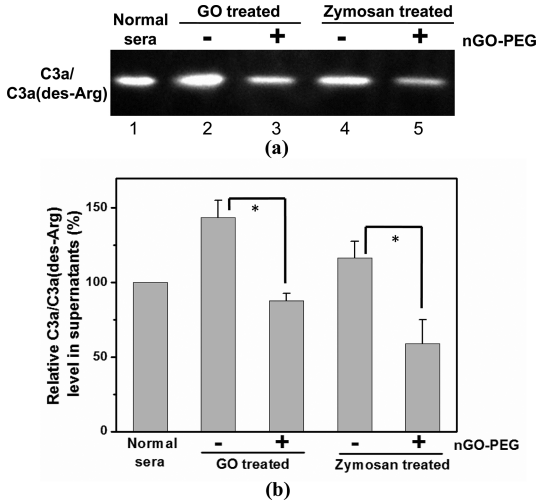

Figure 6. Modulation of the C3a/C3a(des-Arg) level in C3a/C3a(des-Arg)-elevated sera by nGO-PEG treatment. (a) C3a/C3a(des-Arg)-elevated sera were prepared by preincubating normal sera with either 5 mg/mL zymosan or 40 μg/mL unfunctionalized GO, and then incubated with nGO-PEG-conjugated beads (+) and control beads (−), respectively. After removal of the beads, C3a/C3a(des-Arg) remained in the supernatant was analyzed by Western blot. All incubations were carried out at 37 °C. (b) Relative quantification of the western analysis data in a. + corresponds 40 μg/mL beads-conjugated nGO-PEG in the reaction. Error bars represent the standard deviation (n = 3). *P < 0.01.

below the basal level (lane 5), suggesting a potential application of nGO-PEG as an efficient remover for C3a/C3a(des-Arg).

4. CONCLUSION

In this study, we investigated the effects of PEGylation on serum behaviors of GO nanosheets by comparing their interactions with serum proteins. Compared with unfunctionalized GO, nGO-PEG showed dramatic reductions in both protein binding in general and the ability to induce complement C3 cleavage as expected. However, interestingly, both the pull-down assay and subsequent LC-MS/MS data revealed certain selectivity and increased binding capacities of nGO-PEG toward a few serum proteins, six of which were identified, including C3a/C3a(des-Arg), a proinflammatory/obesity-related adipogenic cytokine produced from C3 cleavage during complement activation. A series of Western blot analysis confirmed the high binding capacity of nGO-PEG with C3a/C3a(des-Arg), enabling the former to serve as a potential regulator of the later and its related diseases. Evidently, PEGylation can selectively affect the interactions between GO nanosheets and different serum factors, likely due to the changes of surface chemistry which lead to variations at the nanobio interface. Future work is required to further investigate the selective interactions of nGO-PEG with C3a/C3a(des-Arg) and other serum factors. Given the apparent size difference between nGO-PEG and as made GO, the potential size effect on the above interactions may be investigated as well. Nevertheless, our findings demonstrate an interesting aspect of the changes at the nanobio interface and in serum behaviors of GO nanosheets after PEGylation, and suggest novel potentials of nGO-PEG in biomedical researches as well as in nanobiotechnology. Furthermore, the proof-of-concept demonstration brings up an interesting idea that, when dealing with biocompatibility issues, instead of traditional functionalization strategies, one nanomaterial may be used to help enhance the biocompatibilities of other nanomaterials.

■ ASSOCIATED CONTENT

Supporting Information

Additional characterization data include FT-IR spectra of GO and nGO-PEG and LC-MS/MS raw data. This material is available free of charge via the Internet at http://pubs.acs.org/.

■ AUTHOR INFORMATION

Corresponding Author

*E-mail: zliu@suda.edu.cn; rpeng@suda.edu.cn.

Notes

The authors declare no competing financial interest.

■ ACKNOWLEDGMENTS

This work is supported by the National Basic Research Program of China (973 Program, 2012CB932600 and 2011CB911000), NSFC (51132006, 31070707, 91027039, 51002100), the Research Fund for the Doctoral Program of Higher Education of China (20103201120021), and a project funded by the Priority Academic Program Development of Jiangsu Higher Education Institutions (PAPD).

■ REFERENCES

(1) Ge, C. C.; Du, J. F.; Zhao, L. N.; Wang, L. M.; Liu, Y.; Li, D. H.; Yang, Y. L.; Zhou, R. H.; Zhao, Y. L.; Chai, Z. F.; Chen, C. Y. *Proc. Natl. Acad. Sci. U.S.A.* **2011**, *108*, 16968−16973.
(2) Owens Iii, D. E.; Peppas, N. A. *Int. J. Pharm.* **2006**, *307*, 93−102.
(3) Dobrovolskaia, M. A.; Aggarwal, P.; Hall, J. B.; McNeil, S. E. *Mol. Pharm.* **2008**, *5*, 487−495.
(4) Lynch, I.; Cedervall, T.; Lundqvist, M.; Cabaleiro-Lago, C.; Linse, S.; Dawson, K. A. *Adv. Colloid Interface Sci.* **2007**, *134*−*135*, 167−174.
(5) Dobrovolskaia, M. A.; Aggarwal, P.; Hall, J. B.; McLeland, C. B.; McNeil, S. E. *Adv. Drug Delivery Rev.* **2009**, *61*, 428−437.
(6) Karmali, P. P.; Simberg, D. *Expert Opin. Drug Delivery* **2011**, *8*, 343−357.
(7) Linse, S.; Cabaleiro-Lago, C.; Xue, W.-F.; Lynch, I.; Lindman, S.; Thulin, E.; Radford, S. E.; Dawson, K. A. *Proc. Natl. Acad. Sci. U.S.A.* **2007**, *104*, 8691−8696.
(8) Zhang, D.; Neumann, O.; Wang, H.; Yuwono, V. M.; Barhoumi, A.; Perham, M.; Hartgerink, J. D.; Wittung-Stafshede, P.; Halas, N. J. *Nano Lett.* **2009**, *9*, 666−671.
(9) Karajanagi, S. S.; Vertegel, A. A.; Kane, R. S.; Dordick, J. S. *Langmuir* **2004**, *20*, 11594−11599.
(10) Lynch, I.; Dawson, K. A.; Linse, S. *Sci. STKE* **2006**, *327*, pe14.
(11) Salvador-Morales, C.; Flahaut, E.; Sim, E.; Sloan, J.; Green, M. L. H.; Sim, R. B. *Mol. Immunol.* **2006**, *43*, 193−201.
(12) Zolnik, B. S.; González-Fernández, Á.; Sadrieh, N.; Dobrovolskaia, M. A. *Endocrinology* **2010**, *151*, 458−465.
(13) Xie, J.; Lee, S.; Chen, X. *Adv. Drug Delivery Rev.* **2010**, *62*, 1064−1079.
(14) Sim, R. B.; Tsiftsoglou, S. A. *Biochem. Soc. Trans.* **2004**, *32*, 21−27.
(15) Hawlisch, H.; Wills-Karp, M.; Karp, C. L.; Kohl, J. *Mol. Immunol.* **2004**, *41*, 123−131.
(16) Köhl, J. *Mol. Immunol.* **2001**, *38*, 175−187.
(17) Onat, A.; Can, G.; Rezvani, R.; Cianflone, K. *Clin. Chim. Acta* **2011**, *412*, 1171−1179.
(18) Schraufstatter, I. U.; Trieu, K.; Sikora, L.; Sriramarao, P.; DiScipio, R. *J. Immunol.* **2002**, *169*, 2102−2110.
(19) Oksjoki, R.; Kovanen, P. T.; Pentikainen, M. O. *Curr. Opin. Lipidol.* **2003**, *14*, 477−482.
(20) Haque, R.; Hwang, B. Y.; Appelboom, G.; Piazza, M. A.; Guo, K.; Connolly, E. S. *J. Clin. Neurosci.* **2011**, *18*, 1235−1239.
(21) Szebeni, J. *Toxicology* **2005**, *216*, 106−121.

(22) Kopelevich, Y.; Esquinazi, P. *Adv. Mater.* **2007**, *19*, 4559−4563.
(23) Stankovich, S.; Dikin, D. A.; Dommett, G. H. B.; Kohlhaas, K. M.; Zimney, E. J.; Stach, E. A.; Piner, R. D.; Nguyen, S. T.; Ruoff, R. S. *Nature* **2006**, *442*, 282−286.
(24) Geim, A. K.; Novoselov, K. S. *Nat. Mater.* **2007**, *6*, 183−191.
(25) Jiao, L.; Zhang, L.; Wang, X.; Diankov, G.; Dai, H. *Nature* **2009**, *458*, 877−880.
(26) Loh, K. P.; Bao, Q.; eda, G.; Chhowalla, M. *Nat. Chem.* **2010**, *2*, 1015−1024.
(27) Li, J. H.; Wang, Y.; Li, Z. H.; Wang, J.; Lin, Y. H. *Trends Biotechnol.* **2011**, *29*, 205−212.
(28) Yan, L.; Zheng, Y. B.; Zhao, F.; Li, S.; Gao, X.; Xu, B.; Weiss, P. S.; Zhao, Y. *Chem. Soc. Rev.* **2012**, *41*, 97−114.
(29) Feng, L.; Liu, Z. *Nanomedicine* **2011**, *6*, 317−324.
(30) Liu, Y.; Dong, X.; Chen, P. *Chem. Soc. Rev.* **2012**, *41*, 2283−2307.
(31) Zhang, Y.; Nayak, T. R.; Hong, H.; Cai, W. *Nanoscale* **2012**, *4*, 3833−3842.
(32) Hu, W.; Peng, C.; Luo, W.; Lv, M.; Li, X.; Li, D.; Huang, Q.; Fan, C. *ACS Nano* **2010**, *4*, 4317−4323.
(33) Hong, H.; Yang, K.; Zhang, Y.; Engle, J. W.; Feng, L.; Yang, Y.; Nayak, T. R.; Goel, S.; Bean, J.; Theuer, C. P.; Barnhart, T. E.; Liu, Z.; Cai, W. *ACS Nano* **2012**, *6*, 2361−2370.
(34) He, S. J.; Song, B.; Li, D.; Zhu, C. F.; Qi, W. P.; Wen, Y. Q.; Wang, L. H.; Song, S. P.; Fang, H. P.; Fan, C. H. *Adv. Funct. Mater.* **2010**, *20*, 453−459.
(35) Pei, H.; Li, J.; Lv, M.; Wang, J.; Gao, J.; Lu, J.; Li, Y.; Huang, Q.; Hu, J.; Fan, C. *J. Am. Chem. Soc.* **2012**, *134*, 13843−13849.
(36) Xi, F.; Zhao, D.; Wang, X.; Chen, P. *Electrochem. Commun.* **2012**, *26*, 81−84.
(37) Feng, L.; Wu, L.; Qu, X. *Adv. Mater.* **2013**, *25*, 168−186.
(38) Fisher, C.; Rider, A. E.; Han, Z. J.; Kumar, S.; Levchenko, I.; Ostrikov, K. *J. Nanomater.* **2012**, *2012*, 1−19.
(39) Dong, H.; Zhao, Z.; Wen, H.; Li, Y.; Guo, F.; Shen, A.; Pilger, F.; Lin, C.; Shi, D. *Sci. China Chem.* **2010**, *53*, 2265−2271.
(40) Liu, Z.; Robinson, J. T.; Sun, X. M.; Dai, H. J. *J. Am. Chem. Soc.* **2008**, *130*, 10876−10877.
(41) Zhang, L.; Xia, J.; Zhao, Q.; Liu, L.; Zhang, Z. *Small* **2010**, *6*, 537−544.
(42) Sun, X.; Liu, Z.; Welsher, K.; Robinson, J. T.; Goodwin, A.; Zaric, S.; Dai, H. *Nano Res.* **2008**, *1*, 203−212.
(43) Zhang, W.; Guo, Z.; Huang, D.; Liu, Z.; Guo, X.; Zhong, H. *Biomaterials* **2011**, *32*, 8555−8561.
(44) Feng, L.; Zhang, S.; Liu, Z. *Nanoscale* **2011**, *3*, 1252−1257.
(45) Yang, X. Y.; Zhang, X. Y.; Liu, Z. F.; Ma, Y. F.; Huang, Y.; Chen, Y. *J. Phys. Chem. C* **2008**, *112*, 17554−17558.
(46) Chen, B.; Liu, M.; Zhang, L.; Huang, J.; Yao, J.; Zhang, Z. *J. Mater. Chem.* **2011**, *21*, 7736−7741.
(47) Zhang, L.; Lu, Z.; Zhao, Q.; Huang, J.; Shen, H.; Zhang, Z. *Small* **2011**, *7*, 460−464.
(48) Bao, H.; Pan, Y.; Ping, Y.; Sahoo, N. G.; Wu, T.; Li, L.; Li, J.; Gan, L. H. *Small* **2011**, *7*, 1569−1578.
(49) Yang, X. Y.; Wang, Y. S.; Huang, X.; Ma, Y. F.; Huang, Y.; Yang, R. C.; Duan, H. Q.; Chen, Y. S. *J. Mater. Chem.* **2011**, *21*, 3448−3454.
(50) Huang, P.; Xu, C.; Lin, J.; Wang, C.; Wang, X. S.; Zhang, C. L.; Zhou, X. C.; Guo, S. W.; Cui, D. X. *Theranostics* **2011**, *1*, 240−250.
(51) Markovic, Z. M.; Harhaji-Trajkovic, L. M.; Todorovic-Markovic, B. M.; Kepic, D. P.; Arsikin, K. M.; Jovanovic, S. P.; Pantovic, A. C.; Dramicanin, M. D.; Trajkovic, V. S. *Biomaterials* **2011**, *32*, 1121−1129.
(52) Yang, K.; Zhang, S.; Zhang, G.; Sun, X.; Lee, S.-T.; Liu, Z. *Nano Lett.* **2010**, *10*, 3318−3323.
(53) Robinson, J. T.; Tabakman, S. M.; Liang, Y.; Wang, H.; Sanchez Casalongue, H.; Vinh, D.; Dai, H. *J. Am. Chem. Soc.* **2011**, *133*, 6825−6831.
(54) Tian, B.; Wang, C.; Zhang, S.; Feng, L.; Liu, Z. *ACS Nano* **2011**, *5*, 7000−7009.
(55) Yang, K.; Wan, J.; Zhang, S.; Tian, B.; Zhang, Y.; Liu, Z. *Biomaterials* **2012**, *33*, 2206−2214.
(56) Li, M.; Yang, X.; Ren, J.; Qu, K.; Qu, X. *Adv. Mater.* **2012**, *24*, 1722−1728.
(57) Li, Y.; Liu, Y.; Fu, Y.; Wei, T.; Le Guyader, L.; Gao, G.; Liu, R.-S.; Chang, Y.-Z.; Chen, C. *Biomaterials* **2012**, *33*, 402−411.
(58) Wang, K.; Ruan, J.; Song, H.; Zhang, J. L.; Wo, Y.; Guo, S. W.; Cui, D. X. *Nanoscale Res. Lett.* **2011**, *6*, 8.
(59) Duch, M. C.; Budinger, G. R.; Liang, Y. T.; Soberanes, S.; Urich, D.; Chiarella, S. E.; Campochiaro, L. A.; Gonzalez, A.; Chandel, N. S.; Hersam, M. C.; Mutlu, G. M. *Nano Lett.* **2011**, *11*, 5201−5207.
(60) Yang, K.; Wan, J.; Zhang, S.; Zhang, Y.; Lee, S. T.; Liu, Z. *Acs Nano* **2011**, *5*, 516−522.
(61) Hu, W.; Peng, C.; Lv, M.; Li, X.; Zhang, Y.; Chen, N.; Fan, C.; Huang, Q. *ACS Nano* **2011**, *5*, 3693−3700.
(62) Yan, L.; Zhao, F.; Li, S.; Hu, Z.; Zhao, Y. *Nanoscale* **2011**, *3*, 362−382.
(63) Ruiz, O. N.; Fernando, K. A.; Wang, B.; Brown, N. A.; Luo, P. G.; McNamara, N. D.; Vangsness, M.; Sun, Y. P.; Bunker, C. E. *ACS Nano* **2011**, *5*, 8100−8107.
(64) Singh, S. K.; Singh, M. K.; Kulkarni, P. P.; Sonkar, V. K.; Grácio, J. J. A.; Dash, D. *ACS Nano* **2012**, *6*, 2731−2740.
(65) Jin, L.; Yang, K.; Yao, K.; Zhang, S.; Tao, H.; Lee, S.-T.; Liu, Z.; Peng, R. *ACS Nano* **2012**, *6*, 4864−4875.
(66) Laemmli, U. K. *Nature* **1970**, *227*, 680−685.
(67) Klos, A.; Bank, S.; Gietz, C.; Bautsch, W.; Koehl, J.; Burg, M.; Kretzschmar, T. *Biochemistry* **1992**, *31*, 11274−11282.
(68) Otsuka, H.; Nagasaki, Y.; Kataoka, K. *Adv. Drug Delivery Rev.* **2003**, *55*, 403−419.
(69) Pasut, G.; Veronese, F. M. *J. Controlled Release* **2012**, *161*, 461−472.
(70) Veronese, F. M.; Pasut, G. *Drug Discovery Today* **2005**, *10*, 1451−1458.
(71) Kunzmann, A.; Andersson, B.; Thurnherr, T.; Krug, H.; Scheynius, A.; Fadeel, B. *Biochim. Biophys. Acta* **2011**, *1810*, 361−373.
(72) Moghimi, S. M.; Hunter, A. C.; Murray, J. C. *Pharmacol. Rev.* **2001**, *53*, 283−318.
(73) Sant, S.; Poulin, S.; Hildgen, P. *J. Biomed. Mater. Res.* **2008**, *87A*, 885−895.
(74) Zucker, M. B.; Katz, I. R. *Proc. Soc. Exp. Biol. Med.* **1991**, *198*, 693−702.
(75) Preissner, K. T. *Annu. Rev. Cell Biol.* **1991**, *7*, 275−310.
(76) Jones, S. E.; Jomary, C. *Int. J. Biochem. Cell Biol.* **2002**, *34*, 427−431.
(77) Coughlin, S. R. *Nature* **2000**, *407*, 258−264.
(78) Jones, A. L.; Hulett, M. D.; Parish, C. R. *Immunol. Cell Biol.* **2005**, *83*, 106−118.
(79) Olsen, J. V.; Ong, S.-E.; Mann, M. *Mol.Cell.Proteomics.* **2004**, *3*, 608−614.
(80) Files, J. C.; Malpass, T. W.; Yee, E. K.; Ritchie, J. L.; Harker, L. A. *Blood* **1981**, *58*, 607−618.
(81) Butenas, S.; van't Veer, C.; Mann, K. G. *Blood* **1999**, *94*, 2169−2178.
(82) Hamad, I.; Hunter, A. C.; Rutt, K. J.; Liu, Z.; Dai, H.; Moghimi, S. M. *Mol. Immunol.* **2008**, *45*, 3797−3803.
(83) Reca, R.; Mastellos, D.; Majka, M.; Marquez, L.; Ratajczak, J.; Franchini, S.; Glodek, A.; Honczarenko, M.; Spruce, L. A.; Janowska-Wieczorek, A.; Lambris, J. D.; Ratajczak, M. Z. *Blood* **2003**, *101*, 3784−3793.
(84) Gasque, P.; Singhrao, S. K.; Neal, J. W.; Wang, P.; Sayah, S.; Fontaine, M.; Morgan, B. P. *J. Immunol.* **1998**, *160*, 3543−3554.